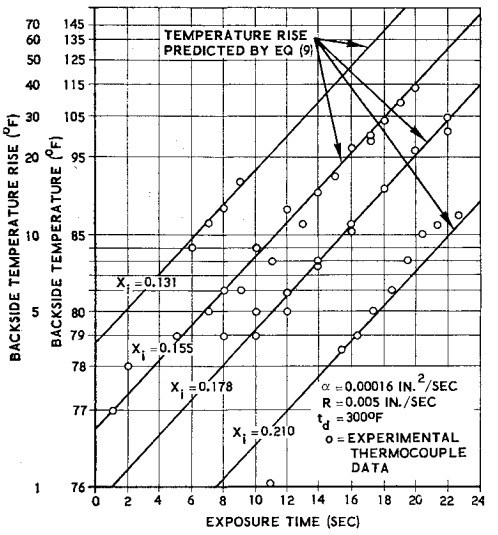

Fig. 2 Comparison of predicted and experimental backside temperatures for various thickness insulators.

Therefore,

$$\partial u/\partial\theta = -R \tag{3}$$

and noting that

$$\partial^2 t/\partial x^2 = \partial^2 t/\partial u^2 \tag{4}$$

and

$$\frac{\partial t}{\partial\theta} = \frac{\partial u}{\partial\theta}\frac{\partial t}{\partial u} + \frac{\partial t}{\partial\theta'}\frac{\partial\theta'}{\partial\theta} \tag{5}$$

with $\partial\theta'/\partial\theta = 1$, substituting Eq. (3) into Eq. (5) gives

$$\frac{\partial t}{\partial\theta} = -R\frac{\partial t}{\partial u} + \frac{\partial t}{\partial\theta'} \tag{6}$$

substituting Eqs. (6) and (4) into Eq. (1) gives

$$\frac{d^2t}{du^2} + \frac{R}{\alpha}\frac{dt}{du} = 0 \tag{7}$$

by noting that $\partial t/\partial\theta' = 0$ in the quasi-steady state. Integration of Eq. (7) and use of semi-infinite boundary conditions, $t \to t_i$ as $u \to \infty$ and $t = t_d$ when $u = 0$, yields the following for the backside temperature rise:

$$t_b - t_i = (t_d - t_i)\exp(-Ru_b/\alpha) \tag{8}$$

Employing Eq. (2), which relates u_b, x_i, and θ, yields the following:

$$t_b - t_i = (t_d - t_i)\exp(-Rx_i/\alpha + R^2\theta/\alpha) \tag{9}$$

By use of Eq. (9), it is possible to estimate the backside temperature rise of an insulator as a function of exposure time for various initial thicknesses in a solid-propellant rocket motor.

The value of t_d, used in Eq. (9), may be determined from experimental data. In this investigation, data showed it to be approximately 300°F. Physically, this value approximates the start of thermal decomposition in silica-filled Buna-N rubber.

In Fig. 2, experimental backside temperature for various exposure times and initial thicknesses are compared with those predicted by Eq. (9). The predicted backside temperatures and the experimental data are in close agreement, within 3°F, at any reported exposure time.

Agreement of the predicted and experimental data indicates that a useful approximate relationship has been developed to estimate rapidly the backside temperature of silica-filled, Buna-N internal insulators in solid-propellant rocket motors. This relationship can be used in design applications for rapid selection of optimum insulator and motor-case thicknesses.

References

[1] Avery, W. H., "Radiation effects in propellant burning," J. Phys. Chem. **54**, 992 (1950).

[2] Eckert, E. R. G. and Drake, R. M., *Heat and Mass Transfer* (McGraw-Hill Book Co., Inc., NewYork, 1959), Chap. 5, p. 110.

[3] Schneider, P. J., *Conduction Heat Transfer* (Addison-Wesley Publishing Co., Inc., Reading, Mass., 1955), Chap. 11, p. 284.

[4] Carslaw, H. C. and Jaeger, J. C., *Conduction of Heat in Solids* (Clarendon Press, Oxford, England, 1959), Chap. 11, p. 282.

Flutter of Multibay Panels at Supersonic Speeds

WILLIAM P. RODDEN*
Aerospace Corporation, El Segundo, Calif.

IN Ref. 1, Dowell has carried out a comprehensive study of the flutter of two-dimensional multibay panels at high supersonic Mach numbers. The stability boundaries presented in Ref. 1 for the two-bay and four-bay configurations differ substantially from earlier results obtained by the present author. Dowell attributes the differences to a lack of convergence related to approximations in the previous collocation (or lumped-parameter) solutions. This was not the case, and it is the purpose of this note to review the difficulties in the previous solutions and to correlate the correctness of Dowell's results by proper application of the collocation method.

The two-bay panel was originally investigated in the author's thesis,[2] and the results have been reported in Refs. 3 and 4; the subsequent investigation of the four-bay panel was reported by Fung[4] in his survey of theories and experiments on panel flutter. The method of analysis was a numerical collocation solution of the aeroelastic integral equation expressed in terms of a structural influence coefficient matrix (SIC), a mass matrix, and an aerodynamic influence coefficient matrix (AIC), which permitted construction of the conventional required damping vs velocity flutter stability curve. The particular collocation formulation was developed in Ref. 5, and the panel AIC's have been reviewed in Ref. 6. The two-bay and four-bay panels are considered in turn in the following, since each encountered a different difficulty in its solution.

In reviewing the two-bay panel calculations, the question of convergence was considered first. In Ref. 2 each bay was divided into ten segments and nine collocation control points, the SIC's and AIC's (including *all* unsteady terms in the panel pressure expression) were generated by desk calculations (the mass matrix was a unit diagonal), and the North American Aviation, Inc., high-speed digital computer program based on Ref. 5 was used for the flutter solution. The present state of automation includes not only a faster and more accurate flutter solution[7] but also programs for the generation, in punched-card format, of SIC's[8] and panel AIC's.[9] It was therefore feasible to attempt verification of the sufficiency of the original 18 degree-of-freedom analysis of the two-bay panel by doubling the number of divisions of each bay (20 segments and 19 control points). The 38 degree-of-freedom analysis demonstrated the adequacy of the original division. It then became necessary to look elsewhere for the source of the discrepancy. It was soon dis-

Received April 6, 1964.

* Manager, Dynamics Section, Aerodynamics and Propulsion Research Laboratory. Associate Fellow Member AIAA.

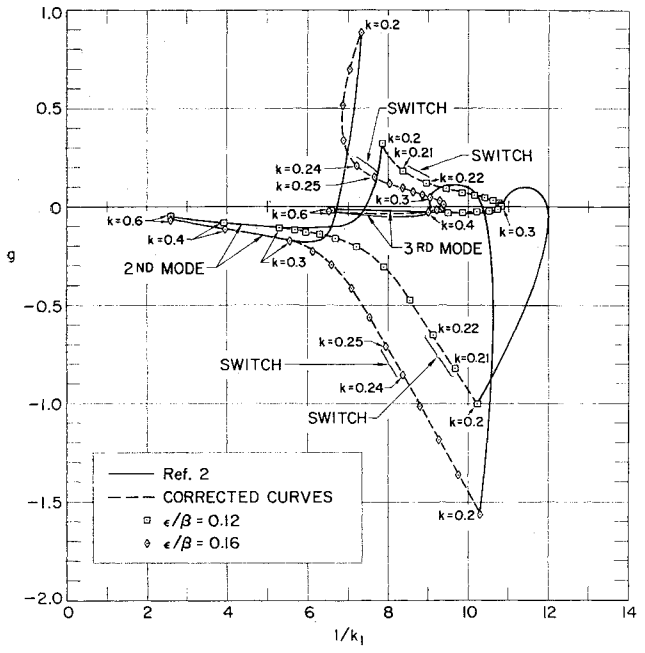

Fig. 1 Flutter stability determination for two-bay panel at $M = 1.56$.

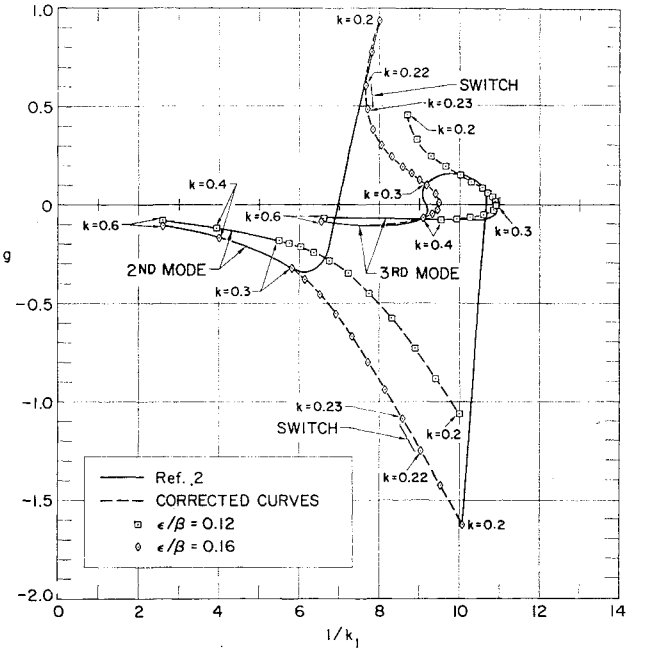

Fig. 2 Flutter stability determination for two-bay panel at $M = 2.00$.

covered, by computing additional points for the stability curves, that the eigenvalues corresponding to the second and third modes which came out of the flutter solution in order at high reduced frequency $k \geq 0.3$ (based on panel semichord) switched between the reduced frequencies of $k = 0.3$ and $k = 0.2$, so that the second eigenvalue at $k = 0.2$ corresponded to the *third* mode, whereas the third eigenvalue corresponded to the *second* mode. This was a consequence of obtaining the complex eigenvalues by the power method (matrix iteration) which yields the eigenvalues in order of descending modulus, but it was not apparent because of the large spacing of the original points. The original and additional points and the original and corrected curves for the second and third modes are shown in Fig. 1 for the Mach number $M = 1.56$ and in Fig. 2 for $M = 2.00$; the notation of the figures uses g for required structural damping coefficient, $1/k_1$ for the reduced velocity based on the fundamental frequency of the panel, ϵ for the mass ratio (product of air density and bay length divided by panel mass per unit length), and $\beta = (M^2 - 1)^{1/2}$. The regions of switching of the order of the eigenvalues are indicated. It is interesting to note that, although the second and third eigenvalues did not switch at $M = 2.00$ for $\epsilon/\beta = 0.12$, the points for $k = 0.2$ were not obtained originally because the iteration solution did not converge; the points were obtained in the recent calculation because the eigenvalue subroutine developed for Ref. 7 accounts for the convergence problems associated with a pair of complex roots having close moduli. The original fairing of the curves was consistent with the limited amount of data, although it may appear somewhat arbitrary in retrospect. It is seen that the third mode rather than the second is the critical flutter mode for the two-bay panel. This agrees with Dowell's general observation that, if there is a sufficient amount of aerodynamic damping, the critical flutter condition for a multibay panel results from coupling of the fundamental mode and the mode that corresponds to the second mode of the one-bay panel [i.e., the $(N + 1)$th mode of an N-bay panel].

The review of the four-bay panel calculations at $M = 2.00$ uncovered a mistake in processing the data for a machine language program.† In reading the AIC's into the computer for the flutter calculations, an incorrect storage location was specified for the first element of one of the rows which consequently rendered the results meaningless for all four values of the reduced frequency originally considered ($k = 0.2$, 0.3, 0.4, and 0.6). The corrected calculations for the critical fifth mode of the four-bay panel are shown in Fig. 3. The curves for the critical modes of Figs. 2 and 3 differ because each bay of the four-bay panel was divided into five segments and four control points in contrast to the ten segments and nine control points in each bay of the two-bay panel; the differences provide a measure of the convergence error of the idealization with only four control points per bay. The restriction of the four-bay analysis to 16 degrees of freedom was necessary because of the limited capacity of the earlier computer (IBM 704), since 36 (nine points per bay) would have exceeded its capacity.‡

The stability boundaries of Figs. 1–3 are compared to Ref. 1 in Fig. 4. The stiffness parameter λ and the aerodynamic damping coefficient g_A of Ref. 1 may be generalized to agree with the first-order unsteady supersonic theory and

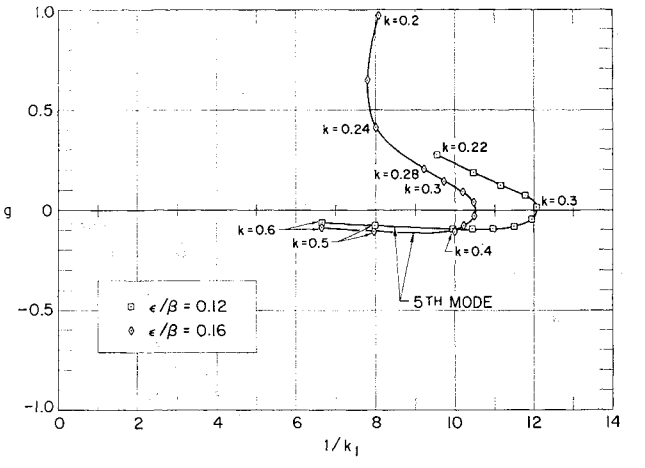

Fig. 3 Flutter stability determination for four-bay panel at $M = 2.00$.

† The new programs of Refs. 7–9 are written in the Fortran language.

‡ The capacity of the IBM 7090 for which Ref. 7 was written now permits 49 degrees of freedom.

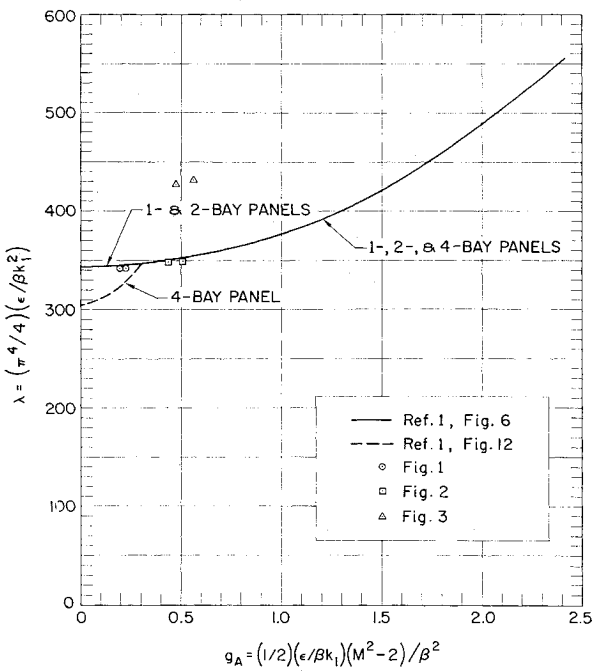

Fig. 4 Comparison of flutter stability boundaries for zero structural damping.

also related to the notation of Ref. 2 through the definitions $\lambda = (\pi^4/4)(\epsilon/\beta k_1^2)$ and $g_A = \frac{1}{2}(\epsilon/\beta k_1)(M^2 - 2)/\beta^2$. The abscissa g_A is shown in Fig. 4 rather than the total damping coefficient g_T of Ref. 1, where $g_T = g_A + g_S$ and g_S is the equivalent viscous structural damping coefficient, because the conventional structural damping can be destabilizing, whereas viscous damping is always stabilizing. The destabilizing effect of structural damping is apparent in Figs. 1–3 from the reversed slope of the critical curves for moderate values of g. This destabilizing effect of structural damping on panel flutter has been analyzed by Johns[10]; certain essentially different properties of viscous and structural dampings were first pointed out by Soroka.[11]

The comparison in Fig. 4 shows excellent agreement between Figs. 1 and 2 and Ref. 1. The 20% discrepancy between Fig. 3 and Ref. 1 measures the convergence error in terms of stiffness requirement of the 16 degree-of-freedom idealization of the four-bay panel. Particularly significant is the agreement between Fig. 1 and Ref. 1, since it indicates that the first-order unsteady aerodynamic theory is valid for panel flutter calculations at supersonic Mach numbers at least as low as $M = 1.56$; the determination of the lower Mach number limit of the first-order unsteady theory is one of the subjects of the current investigation on multibay panels in Ref. 9.

References

[1] Dowell, E., "The flutter of multi-bay panels at high supersonic speeds," Massachusetts Institute of Technology ASRL TR 112-1, Air Force Office of Scientific Research (AFOSR) 5327 (August 1963); also AIAA Preprint 64-92 (January 1964).

[2] Rodden, W. P., "The flutter of two-dimensional flat panels with equally spaced supports in a supersonic flow," Ph.D. Thesis, Univ. of California, Los Angeles, Calif. (October 1, 1957).

[3] Miles, J. W. and Rodden, W. P., "On the supersonic flutter of two-dimensional infinite panels," J. Aerospace Sci. **26**, 190–191 (1959).

[4] Fung, Y. C. B., "A summary of the theories and experiments on panel flutter," California Institute of Technology, Air Force Office of Scientific Research AFOSR TN 60-224 (May 1960).

[5] Rodden, W. P., "A matrix approach to flutter calculations," North American Aviation, Inc., NA-56-1070 (May 1, 1956); also IAS Sherman M. Fairchild Fund Paper FF-23 (May 1958).

[6] Rodden, W. P. and Revell, J. D., "The status of unsteady aerodynamic influence coefficients," IAS Sherman M. Fairchild Fund Paper FF-33 (January 23, 1962).

[7] Rodden, W. P., Farkas, E. F., and Malcom, H. A., "Flutter and vibration analysis by a collocation method: analytical development and computational procedure," Aerospace Corp. Rept. TDR-169(3230-11)TN-14 (July 31, 1964).

[8] Rodden, W. P., Farkas, E. F., Commerford, G. L., and Malcom, H. A., "Structural influence coefficients for a redundant system including beam-column effects: analytical development and computational procedure," Aerospace Corp. Rept. (to be published).

[9] Lock, M. H., Rodden, W. P., Farkas, E. F., and Malcom, H. A., "The flutter of two-dimensional, multiple bay, flat panels at low supersonic speeds," Aerospace Corp. Rept. (to be published).

[10] Johns, D. J. and Parks, P. C., "Effect of structural damping on panel flutter," Aircraft Eng. **32**, 304–308 (1960).

[11] Soroka, W. W., "Note on the relations between viscous and structural damping coefficients," J. Aerospace Sci. **16**, 409–410, 448 (1949).

Shock Interaction in a Hypersonic Flow

FRANK R. TEPE JR.* AND WIDEN TABAKOFF†
University of Cincinnati, Cincinnati, Ohio

Nomenclature

δ	= flow deflection angle
ϵ	= angle of the contact surface with respect to the freestream flow direction
P	= static pressure
θ	= shock wave angle
M	= Mach number
δ_b	= wedge body angle
α	= angle of attack of wedge body
$d\delta^*/dx$	= slope of mass boundary layer
T	= static temperature
T_b	= wedge body temperature
μ	= viscosity
μ_b	= viscosity at surface of wedge
Re_x	= Reynolds number at point of interaction

Subscripts

0	= freestream conditions
1	= conditions in region 1 as specified by Fig. 1
2	= conditions in region 2 as specified by Fig. 1
3	= conditions in region 3 as specified by Fig. 1
4	= conditions in region 4 as specified by Fig. 1

Introduction

THE interaction of oblique shock waves of different intensities in a hypersonic flow was investigated from both the theoretical and experimental viewpoints. The angle, with respect to the freestream flow direction, of the vortex layer or contact surface generated by this interaction phenomena is predicted using first an assumption of inviscid flow and then an assumption of viscous flow. Empirical solutions are also developed to predict the angle of the contact surface with a minimum of computation if a high degree of accuracy is not required. The effect of varying the flow and geometric parameters on the viscous solution was also considered.

Although innumerable reports have been published on the theory of shock waves in a supersonic flow, there appears to be very little work accomplished in the field of interaction of oblique shock waves of different families. A study was con-

Received April 6, 1964; revision received May 11, 1964. This research was supported by the U. S. Air Force under Contract AF 33 (616) 8453, monitored by the Aerospace Research Laboratories of the Office of Aerospace Research. The experimental work was conducted in the 20-in. hypersonic wind tunnel of the Aerospace Research Laboratories.

* Research Assistant, Department of Aerospace Engineering.

† Associate Professor, Department of Aerospace Engineering. Member AIAA.